

# Optimization of a Blood Pool Contrast Agent Injection Protocol for MR Angiography

Philippe Robert, PhD,<sup>1\*</sup> Xavier Violas, RT,<sup>1</sup> Robin Santus, RT,<sup>1</sup>  
Denis Le Bihan, MD, PhD,<sup>2</sup> and Claire Corot, PharmD, PhD<sup>1</sup>

**Purpose:** To design an ideal first-pass profile for MR angiography (MRA) by optimizing a multiphasic injection protocol based on two experimental animal models.

**Materials and Methods:** An equivalent contrast-enhanced (CE) MRA injection protocol was developed with controlled injection modalities (injection rate, volume, and dose) in rabbits and pigs. P792, a blood pool contrast agent, was injected in 17 male New Zealand rabbits and five farm pigs with variable injection schemes (mono- and multiphasic). From the gadolinium (Gd) blood concentration data, a simulation of an MR acquisition was performed to evaluate the impact of such an injection protocol on MR arterial signal and to select the best injection protocol.

**Results:** An empirical relationship between the arterial peak concentration and the injection parameters was found in the rabbits and pigs, allowing precise prediction of the first-pass profile. Of the four injection scheme strategies tested (standard bolus and bi-, tri-, and multiphasic injection protocols), the multiphasic “ramp” injection protocol provided the most optimal contrast agent pharmacokinetics with a durable plateau of concentration.

**Conclusion:** Ramp injection protocol provides an optimized first-pass profile for CE-MRA.

**Key Words:** blood pool agents; MR angiography; injection protocol; animal model; pharmacokinetic

**J. Magn. Reson. Imaging 2005;21:611–619.**

© 2005 Wiley-Liss, Inc.

PARAMAGNETIC CONTRAST AGENTS improve the quality and reproducibility of magnetic resonance angiography (MRA), particularly in terms of signal-to-noise ratio (SNR) increase, scan time reduction, and flow dependency (1). Contrast-enhanced (CE) MRA is now a routine clinical examination for many branches of the vascular tree from the thoracic aorta to peripheral arteries.

Because of heart and respiratory movements, CE-MRA of the coronary arteries requires a drastic de-

crease in blood T1 (2). This can be achieved by the rapid injection of a large dose of a nonspecific contrast agent (NSA), such as gadolinium (Gd)-DOTA or Gd-DTPA. However, these injection protocols result in a very sharp bolus with marked T1 variations during the k-space sampling, resulting in image artifacts (3,4). Moreover, the use of NSAs for coronary MRA is already known to induce myocardial enhancement due to extravasation through the capillary wall, leading to decreased contrast between the coronary arteries and surrounding myocardial tissue (5,6). In this context, the ideal bolus profile should be a long plateau with a constant low T1, without any extravasation into the myocardium.

The influence of injection parameters on the bolus profile has been widely studied in CT (7–13) and MRI (14–20). Prediction of the bolus profile is important, and depends on physiologic factors such as cardiac output (CO) and patient age, or experimental factors such as injection rate, contrast agent, and saline flush volume. Mathematical models have been developed that mimic the cardiovascular system and integrate both physiological characteristics and injection parameters (11,13). A good correlation between the first-pass profile predicted by the model and experimental data obtained in patients was found. With this tool, Bae et al (9) demonstrated with a standard CT contrast agent that an optimized injection protocol with multiphasic injection schemes could provide a constant plateau during the first pass. However, the important extravasation of small Gd chelates during the first pass compared to blood pool agents (21) should be a limitation with multiphasic injection protocols. Therefore, the aims of this study were to 1) obtain the optimum first-pass bolus profile with a blood pool contrast agent by investigating different injection protocols (mono-, bi-, and multiphasic) in two different species (rabbit and pig), and 2) evaluate the impact of such injection protocols on the MR blood signal.

## MATERIALS AND METHODS

### Products

P792 (gadomelitol, Vistarem®; Guerbet, Roissy, France) is a high-relaxivity, mono-Gd rapid clearance blood pool contrast agent (RCBPA). This contrast agent has a high molecular volume (5 nm diameter vs. 0.9 nm for conventional NSAs), which drastically decreases its rate

<sup>1</sup>Guerbet Research, Roissy, France.

<sup>2</sup>Service Hospitalier Frédéric Joliot, CEA, Orsay, France.

Presented in part at the 9th Annual Meeting of ISMRM, Glasgow, Scotland, 2001. Poster #1953.

\*Address reprint requests to: P.R., Guerbet, Research Department, B.P. 57400, 95943, Roissy, Charles De Gaulle Cedex, France.  
E-mail: philippe.robert@guerbet-group.com.

Received June 29, 2004; Accepted February 1, 2005.

DOI 10.1002/jmri.20324

Published online in Wiley InterScience (www.interscience.wiley.com).

Table 1  
Injection Modalities for Rabbit Studies

Rabbit number	Product (Dose, mmol/kg)	Injection rate (mL/s)	Volume (mL)	Total Duration (s)
1	Gd-DOTA (0.3)	0.5	0.6	1.2
2	Gd-DOTA (0.3)	0.25	0.6	2.4
3	Gd-DOTA (0.3)	0.13	0.6	4.6
4	Gd-DOTA (0.3)	0.08	0.6	7.5
5, 6, 7	Gd-DOTA (0.1)	0.5	0.5	1
8, 9, 10	P792 (0.013)	0.5	1.1	2.2
11, 12, 13	P792 (0.013)	0.2	1.3	6.5
14, 15	P792 (0.014)	Dose/3 at 0.3 mL/s + dose/3 at 0.15 mL/s + dose/3 at 0.05 mL/s	3.6	36
16, 17	P792 (0.0175)	Decreasing injection rate from 0.25 mL/s (4s) to 0.015 mL/s in 30 sec	4.5	30

of extraction by slowing diffusion through the capillaries (22–24). In addition to this blood pool property, P792 is rapidly cleared by the kidneys. In this study, P792 was tested at 0.013–0.026 mmol Gd/kg with different injection schemes. Gd-DOTA (Dotarem®; Guerbet), a conventional NSA, was used at 0.1–0.3 mmol Gd/kg as the reference product.

### Animal Preparation

All of the animal experiments were performed in compliance with the EEC directive (86/609/EEC) on animal welfare. Seventeen male New Zealand rabbits (mean weight = 3 kg; Wiss Gérard, Saintes Savine, France) and five farm pigs (mean weight = 30 kg; Earl de Frenelle, Charles River, France) were studied using variable injection schemes. All experiments were carried out under general anesthesia. For the rabbits, this was performed by intramuscular injection of ketamine 50 mg/kg and xylazine 0.5 mL/kg. For the pigs, after premedication by intramuscular injection of atropine 0.04 mg/kg, ketamine 12 mg/kg and droperidol 0.4 mg/kg, general anesthesia was obtained by inhalation of 0.5–2% of isoflurane (Forene®) mixed with O<sub>2</sub> (0.6 liter/minute) and N<sub>2</sub>O (0.8 liter/minute). Assisted respiration (8 liter/minute) in the pigs was performed at a rate of 14 cycles/minute with a respirator (Minerve Alpha 100). The marginal ear vein in the rabbits and the jugular vein in the pigs were catheterized for contrast media injection. The pigs were perfused with glucose 5% (30 mL/hour) to compensate for blood volume depletion induced by sampling.

### Injection Protocol and Blood Gd Concentration Measurements

A rapid blood-sampling model, which was initially developed in the rabbit (14), was used in the rabbit and pig to evaluate the experimental parameters governing the bolus phase. With this model we tested P792, using Gd-DOTA as the reference product. An equivalent CE-MRA injection protocol was achieved with controlled injection modalities (injection rate, volume, and dose) in rabbits and pigs. Injections were performed with automatic injectors (Prolabo SAGE® M362 for rabbits, and Angiomat®3000 for pigs). Blood samples (300 µL) were continuously withdrawn from the femoral artery over 45–60 seconds with a time resolution of ~1 sec-

ond. The Gd concentration of these blood samples was measured using an inductively coupled plasma atomic emission spectrometer (ICP-AES). In the case of multiple injections in the same animal, the Gd concentration was corrected by subtracting the residual baseline Gd concentration.

### Monophase Injection Schemes

Experiments were performed with a conventional bolus injection of a standard NSA to compare the two species and the two products. First, 0.1 or 0.3 mmol Gd/kg of Gd-DOTA was injected at different injection rates in each species. The injection rates were chosen with respect to the differences in the COs of the two species compared to humans (CO = ~0.8 ± 0.2 liter/minute in rabbits, ~3.1 ± 0.9 liter/minute in pigs (25), and ~6.5 ± 0.5 liter/minute in humans (26)). Second, Gd-DOTA and P792 pharmacokinetics were compared for one minute in rabbits after injection at 0.5 mL/second of 0.1 mmol Gd/kg and 0.013 mmol Gd/kg, respectively.

### Multiphase Injection Schemes

Biphasic, triphasic, and ramp injection protocols were achieved in rabbits and pigs. Assuming that a high and durable contrast agent concentration during the first pass is favorable for extravasation, we only investigated multiphase injection schemes with P792, which was selected for its limited extravasation.

All of the injection modalities used in this study are summarized in Tables 1 and 2.

### Empirical Correlation

In addition, all the data produced in our laboratory in these animal models, including data beyond the scope of this study, were analyzed empirically to find a potential correlation between the injection parameters (injection rate, contrast media concentration, injection duration, etc.), the species (rabbit and pig), and the first-pass profile. Therefore, the maximum concentration (C<sub>max</sub>) was measured for 40 first-pass experiments in rabbits (25 Gd-DOTA injections and 15 P792 injections) and 21 first-pass experiments in pigs (11 Gd-DOTA injections and 10 P792 injections). These experiments were performed with variable injection schemes (i.e.,

Table 2  
Injection Modalities for Pig Studies

Pig number	Injection order	Product (Dose, mmol/kg)	Injection rate (mL/s)	Volume (mL)	Total Duration (s)
1	1	Gd-DOTA (0.1)	2	6	3
1	2	Gd-DOTA (0.1)	1	6	6
1	3	Gd-DOTA (0.1)	0.5	6	12
1	4	Gd-DOTA (0.1)	0.2	6	30
2	3	P792 (0.013)	2 mL/s (1s) then 0.3 mL/s	12	34
2	4	P792 (0.013)	1 mL/s (6s) then 0.2 mL/s	12	36
2	5	P792 (0.026)	1 mL/s (during 8 sec) followed by a constant decrease from 1 to 0.5 mL/s	24	30
2	6	Gd-DOTA (0.1)	1	6	6
3, 4, 5	1	P792 (0.013)	1	11	11

variable dosages and injection rates) to obtain multiple time-resolved arterial profiles. Since  $C_{max}$  was considered to be independent of the size of the contrast agent (14), the two compounds (P792 and Gd-DOTA) were included indifferently in the analysis.

**Modelization of the First-Pass Pharmacokinetics**

The first-pass pharmacokinetics of the contrast agent were simulated according to the compartmental model proposed by Bae et al (9). This model gives a good approximation of the aortic concentration profile following an intravenous injection (Fig. 1). Equations were solved numerically with Matlab® software (MathWorks, Inc.) for a given injection rate protocol. We investigated the validity of this pharmacokinetic simulation in our animal models by comparing the prediction of arterial concentration with experimental data obtained using the different injection protocols in the two animal species.

**Simulation of the First-Pass MR Signal**

Using these concentration data simulations and the P792 relaxivity constants, we calculated the steady-state MR signal intensity for a standard spoiled gradient-echo sequence at each time-point of the pharmacokinetic profile according to:

$$\frac{M_{xy}}{M_0} = \frac{1 - e^{-TR(\frac{1}{T_{10}} + r_1[Gd])}}{1 - \cos(\alpha) \cdot e^{-TR(\frac{1}{T_{10}} + r_1[Gd])}} \cdot \sin(\alpha) \cdot e^{-\frac{TE}{T_2}(\frac{1}{T_{20}} + r_2[Gd])} \tag{1}$$

T1 and T2 values over the entire pharmacokinetic profile were calculated with the formula  $1/T_{1,2} = 1/T_{10,20} + r_{1,2} \times [Gd]$  ( $T_{10}/T_{20} = 1200/200$  msec for blood,  $r_1/r_2 = 29/65 \text{ s}^{-1} \cdot \text{mM}^{-1}$  at 60 MHz, 37°C in 4%

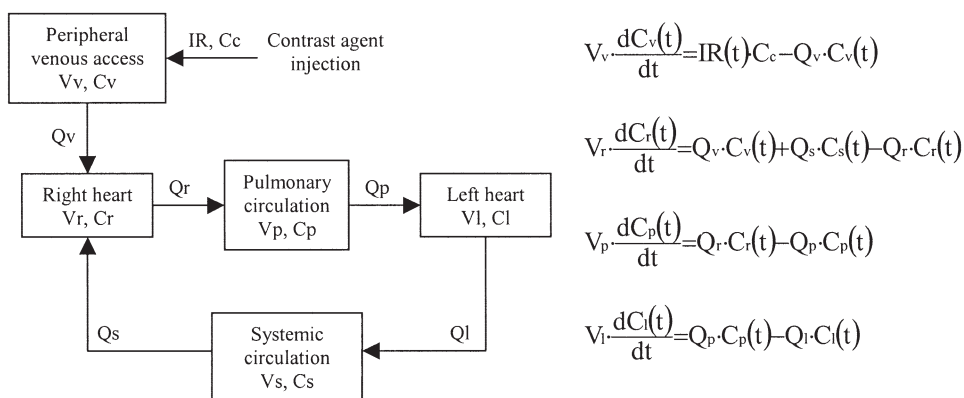


**Figure 1.** Modelization of the arterial first pass (from Ref. 9). Cc corresponds to the concentration of the injected contrast agent; Cv, Cr, Cp, Cl, and Cs are the concentrations in the peripheral venous compartment, right ventricle, pulmonary circulation, left ventricle, and systemic circulation, respectively; IR is the volumic injection rate;  $Q_r = Q_p = Q_l = Q_s$  correspond to the systemic CO;  $Q_v$  is the volumetric flow rate of blood leaving the peripheral vein; Vl, Vp, Vr, Vs, and Vv are the volume of blood in the left heart, blood and interstitial space in the pulmonary compartment, blood in the right heart, blood and interstitial space in the systemic circulation, and blood in the peripheral vein, respectively. This model hypothesizes that 1) the compartment volumes are constant with time, 2) the initial conditions are  $C_v(0) = C_p(0) = C_l(0) = C_s(0) = 0$ , and 3) the flow rates are equivalent to the systemic CO  $Q$ :  $Q_r = Q_p = Q_l = Q_s = Q$ . The concentration time-resolved profile in the arteries corresponds to the concentration in the left ventricle Cl(t).

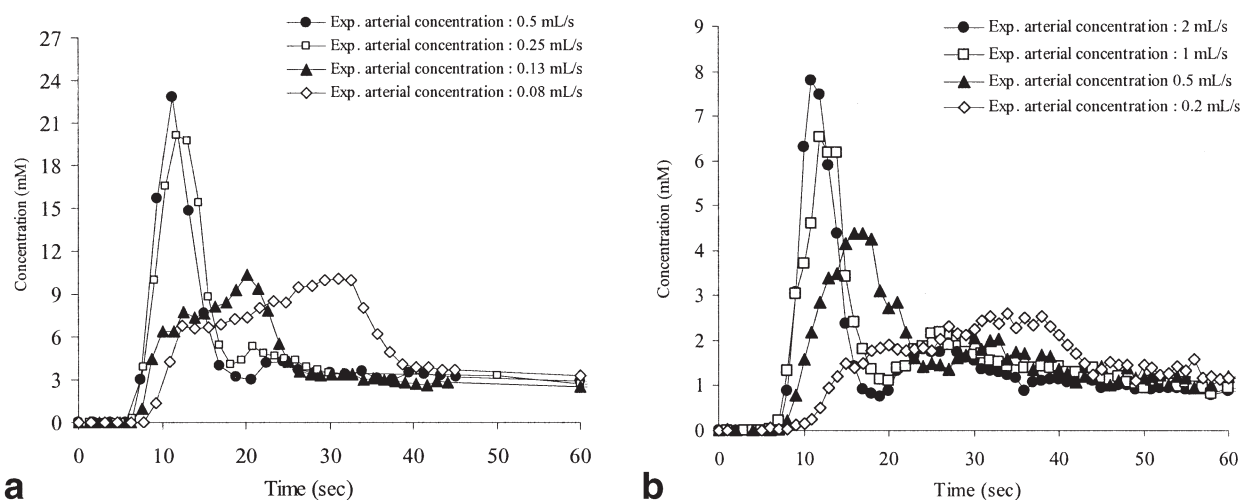


**Figure 2.** First-pass concentration profile as a function of time in rabbits and pigs after injection of Gd-DOTA (500 mM). The  $C_{max}/dose$  at the peak bolus is comparable between the two species when a ratio of 4 between the injection rates is respected. According to the COs of the two species ( $CO = \sim 0.8$  liter/minute in rabbits,  $\sim 4$  liter/minute in pigs), a ratio of 5 should be optimal. **a:** Bolus injection at 0.3 mmol/kg in rabbits with variable injection rates of 0.08–0.5 mL/second. **b:** Bolus injection at 0.1 mmol/kg in pigs with variable injection rates of 0.2–2 mL/second.

HSA). The sequence parameters were  $TR/TE = 5.0/1.5$  msec, flip angle =  $\alpha = 30^\circ$ ,  $N = 512$  phase-encoding steps. With 32 slices, this MR protocol would result in an acquisition time of 82 seconds. Considering that a low TE minimizes the susceptibility artifacts,  $T2^*$  effects were assumed to be proportional by a factor of  $\beta = 0.85$  to  $T2$  (17).

## RESULTS

### Monophase Injection Schemes

The bolus profiles were comparable between the two species (Fig. 2), as expected by the choice of injection rates. The increase in the injection rate (keeping dose and injected volume constant) increases the bolus peak ( $C_{max}$ ) in pigs as well as in rabbits, and decreases the time necessary to reach the maximum concentration.

With a monophase injection scheme, the bolus phase (sharp peak) and postbolus phase (exponential decrease) occurred at different time windows (Fig. 2). The first-pass concentration increases are identical for both contrast agents in the arterial system ( $\sim +570\%$ ) leading to a  $\sim 30$  msec blood  $T1$  (Table 3). However, one minute after injection,  $85\% \pm 8\%$  of the injected P792 remains in the blood pool, compared to only  $37\% \pm 2\%$  for Gd-DOTA (Table 3).

### Prediction of the $C_{max}$ by Empirical Correlation

All of the data obtained in our laboratory were compiled in this first-pass Gd measurement model. An empirical relation between the injection conditions and the maximum concentration at the peak bolus was calculated for each species. There is a strong linear relation between the maximum concentration at the peak bolus and a hybrid parameter constituted by the injection rate and the concentration of the injected solution. Linear regression was calculated between  $Q\gamma$ , which corresponds to the quantity of contrast media injected during the first  $\gamma$  seconds of the injection protocol, and  $C_{max}$ . Using this empirical model,  $C_{max}$  is linearly correlated with the quantity of contrast agent injected in the first  $\gamma = 4$  seconds in rabbits, and the first  $\gamma = 7$  seconds in pigs (Fig. 3).

### Multiphase Injection Schemes

The multiphase injection scheme improves the pharmacokinetic profiles in rabbits (Fig. 4b) and pigs (Fig. 5b and c) according to the targeted concentration plateau. After the bolus phase, the concentration of contrast agent is higher than that in a monophase injection protocol, but the plateau is not achieved. However, when a constant decreased injection scheme is used,

Table 3

Concentration and  $T1$  Results after bolus injection of 0.1 mmol/kg of Gd-DOTA on 0.013 mmol/kg of P792.  $C_0$  is calculated as the resulting concentration if the whole dose was instantaneously diluted in the blood volume (60mL/kg).

		Gd-DOTA	P792
Bolus	$C_{max}$ (mM)	$9.5 \pm 0.4$	$1.4 \pm 0.2$
	$T_{1(\text{peak})}$ (ms)	$29 \pm 2$	$24 \pm 3$
	$C_{max}/C_0$ (%)	$573 \pm 26$	$565 \pm 69$
Post bolus	$C_{60s}$ (mM)	$0.77 \pm 0.05$	$0.24 \pm 0.01$
	$T_{1(60s)}$ (ms)	$340 \pm 10$	$143 \pm 9$
	$C_{60s}/C_0$ (%)	$37 \pm 2$	$85 \pm 8$

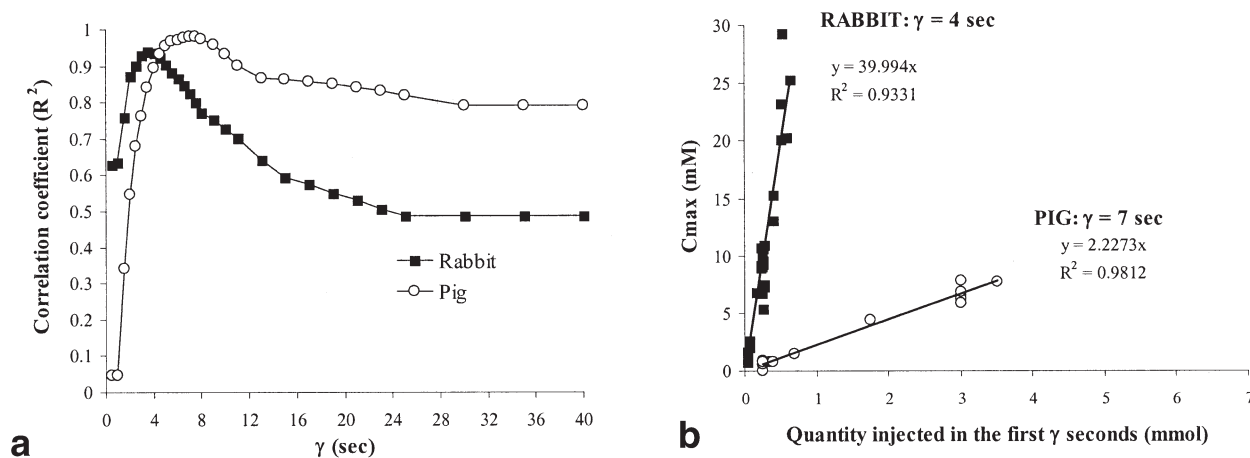


**Figure 3.** Correlation in rabbits and pigs between the quantity  $Q_\gamma$  of molecules injected in the first  $\gamma$  seconds and the maximum concentration  $C_{max}$  observed in the arterial compartment during the bolus. **a:** Correlation coefficient  $R^2$  (between  $C_{max}$  and  $Q_\gamma$ ) as a function of  $\gamma$ : determination of the  $\gamma$  delay optimizing the  $C_{max}$  prediction. **b:** Correlation between the quantity of molecules injected in the first  $\gamma$  seconds and the maximum concentration.

there is a compensation for the clearance of the product, and plateaus in the rabbit (Fig. 4c) and in the pig (Fig. 5d) are achieved. The ramp protocol in the pig was designed with the empirical correlation coefficient found previously (Fig. 3): a first short bolus phase is added prior to the ramp protocol to reach the arterial concentration at the required level ( $T1 = <100$  msec). An increase in the dose (from 0.013 to 0.026 mmol Gd/kg in pigs, and from 0.014 to 0.0175 mmol Gd/kg in rabbits) is therefore necessary for this injection protocol to reach the targeted  $T1$ . The calculated  $T1$  is therefore  $<80$  msec for  $>20$  seconds in rabbits, and  $<100$  msec for 40 seconds in pigs with P792 (Fig. 6). Therefore, in the two species the ramp injection scheme (i.e., injection with a constant decrease in the injection rate) provides a long plateau with a durable low blood  $T1$ .

#### Simulation of First-Pass Pharmacokinetics

All of the injection schemes are well correlated with the mathematical simulation of the first pass for both species (Figs. 4 and 5). Constants of the model were adjusted with respect to the range of published physiological pig data (3,26,27). A time delay of 7 seconds in the pig and 5 seconds in the rabbit was necessary to fit the model to the experimental data.

#### Impact on the MR Signal

In a standard bolus injection protocol, the maximum concentration at the peak bolus ( $C_{max}$ ) differs between the two products in the range of the injected doses (Table 3). As a direct consequence, expressed in  $T1$ , high relaxivity of P792 injected at 0.013 mmol Gd/kg leads to an equivalent  $T1$  decrease down to  $\sim 30$  msec compared to Gd-DOTA injected at 0.1 mmol Gd/kg (Table 3).

In the ramp injection protocol, the strong and stable reduction in the blood  $T1$  (Fig. 6a and b) will lead to a long and durable MR signal enhancement, whereas the standard injection rate scheme at the same dosages would result in a high but variable enhancement in

both species (Fig. 7a and b). A simulation of a bolus protocol at the high dosage was added to the graph to facilitate comparison between the different injection protocols.

#### DISCUSSION

These rabbit and pig experiments demonstrate that the choice of adapted injection rates with respect to the difference in COs makes the bolus profiles very comparable between the two species (Fig. 2). The reproducibility of this model between species suggests that the results could be extrapolated to humans. They also show the lower extravasation of P792 during the first minute postinjection compared to Gd-DOTA. This indicates that a blood pool agent such as P792 is well adapted to an imaging window higher than 15–20 seconds, thanks to limited extravasation.

From this model, we found an empirical correlation between both species that gives the maximum concentration at the peak bolus as a function of the injection conditions (Fig. 3). This simple linear and reproducible relation provides an important guideline for injection rate and dose optimization. We can now distinguish two phases in the injection scheme: the “bolus” phase, which corresponds to the part of the product dose injected before the  $\gamma$  value of the considered species (4 seconds for rabbit, 7 seconds for pigs), and the “infusion” phase, which is all the remaining product injected subsequently. The bolus phase can be considered as a “loading” period during which the injected dose generates the level of the first pass and defines the arterial peak concentration ( $C_{max}$ ). After that, the remaining contrast agent administered defines the infusion period, which in turn governs the plateau duration. In other words, reaching a targeted  $C_{max}$  depends on the dose, the injection rate, and the initial contrast agent concentration via the quantity injected in the first  $\gamma$  seconds. Using this empirical model, the quantity needed during the “bolus loading phase” to achieve the targeted peak concentration can be predicted. For example, a targeted  $C_{max}$  of 0.5 mM in pigs with P792

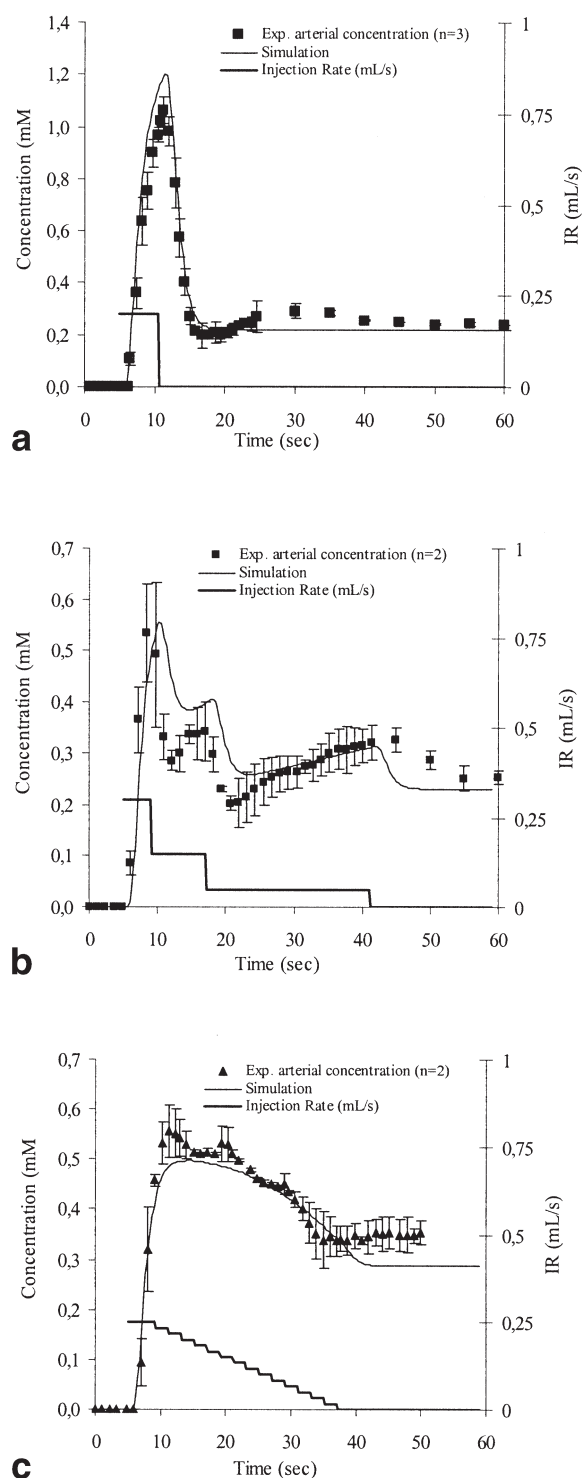


**Figure 4.** First-pass concentration profile as a function of time in rabbits after injection of P792 (**a** and **b**: 13  $\mu\text{mol/kg}$ ; **c**: 17.5  $\mu\text{mol/kg}$ ). Fitted input data: rabbit  $\text{CO} = 6.0$  mL/second,  $V_s = 56.8$  mL/kg,  $Q_v = 0.92$  mL/second,  $C_s = 35$  mM (**a**) and 11.6 mM (**b** and **c**),  $V_v/V_d/V_p/V_g = 0.5/3.3/7.9/3.3$  mL. An added delay of 5 seconds for the simulated protocol was necessary to fit the curve in the time axis. **a**: Bolus injection of P792 (35 mM): 0.2 mL/second over 6.5 seconds. **b**: Biphasic injection protocol of P792 (11.6 mM): 0.3 mL/second over 4 seconds, followed by 0.15 mL/second over 8 seconds, followed by 0.05 mL/second over 24 seconds. **c**: Ramp injection protocol of P792 (11.6 mM): 0.25 mL/second over 4 seconds followed by a ramp of constant decrease from 0.25 to 0.017 mL/second in 2-second steps.

(corresponding to  $T_1 = 65$  msec, with  $r_1 = 29 \text{ s}^{-1} \cdot \text{mM}^{-1}$  and  $T_{10} = 1.2$  seconds) would require an injection of 224  $\mu\text{moles}$  of Gd in the first 7 seconds, leading to an injection rate of  $\text{IR} = 32 \mu\text{mol Gd/second} = 0.9 \text{ mL/second}$  (Fig. 5a). The remaining contrast agent would extend the bolus shape, but would not increase the  $C_{\text{max}}$ .

This empirical relationship between  $C_{\text{max}}$  and the injection parameters was used as a tool for designing an optimal injection protocol. We first showed that a monophasic injection rate induces a sharp, short first-pass profile, which is not well adapted to an MR examination (3). By decreasing the injection rate, we found that a slow, monophasic injection scheme induces a first-pass profile that is flatter than that obtained with a rapid injection rate, but rises slightly (Fig. 2). This result is consistent with previous works (28,29) and suggests that the contrast agent dose is not distributed evenly over the duration of the injection. This nonlinear relationship was also demonstrated in a previous study in humans, where it was observed that an injection rate higher than 8 mL/second does not lead to a significantly greater degree of enhancement in the arterial system (7). This can be explained by the buffer effect of the lung. To resolve this, as proposed by Hittmair et al (8) for X-ray imaging, we tested bi- and triphasic injection schemes. Although this improves the first-pass concentration profile, it still gives a variable arterial curve that is very sensitive to the two or three phase steps. Finally, we demonstrated that a plateau of concentration can be achieved by progressive modulation of the injection rate in rabbits and pigs. The ramp injection protocol results in a constant and high concentration of contrast agent during the first pass. To reach the targeted  $T_1$  in the arterial compartment, this multiphasic injection scheme requires a minimal P792 dose of 0.026 mmol Gd/kg, which represents a fourfold lower Gd dosage compared to standard NSAs.

Previous patient studies have shown that prediction of the bolus profile is important for human applications (15). To address this issue in the current study, we used the model proposed by Bae et al (9) for an approximation of first-pass pharmacokinetics. This linear multi-compartmental model is in good agreement with our experimental data. Adjustments of the flow constants and compartment volumes were necessary to fit the experimental data. Under our conditions, the fitted values for animal physiological constants were found in the range of published data (9,25,27). Additional delays of 5 seconds in rabbits and 7 seconds in pigs were necessary to adjust the time axis, probably because of the long distance between the injection site (ear vein for rabbit and jugular vein for pig) and the sample collection site (femoral artery). However, this model cannot give an analytical equation for predicting the  $\gamma$  value in each species. Indeed, it is not possible to model the nonlinear phenomenon we observed in rabbits and pigs (i.e., proportionality between  $C_{\text{max}}$  and the quantity injected during the  $\gamma$  first seconds) with the theoretical model of first-pass pharmacokinetics, which is linear. The Bae et al (9) model describes the evolution of concentrations in the various compartments using first-order differential equations. With this type of model, the higher the dose injected, the greater the arterial peak

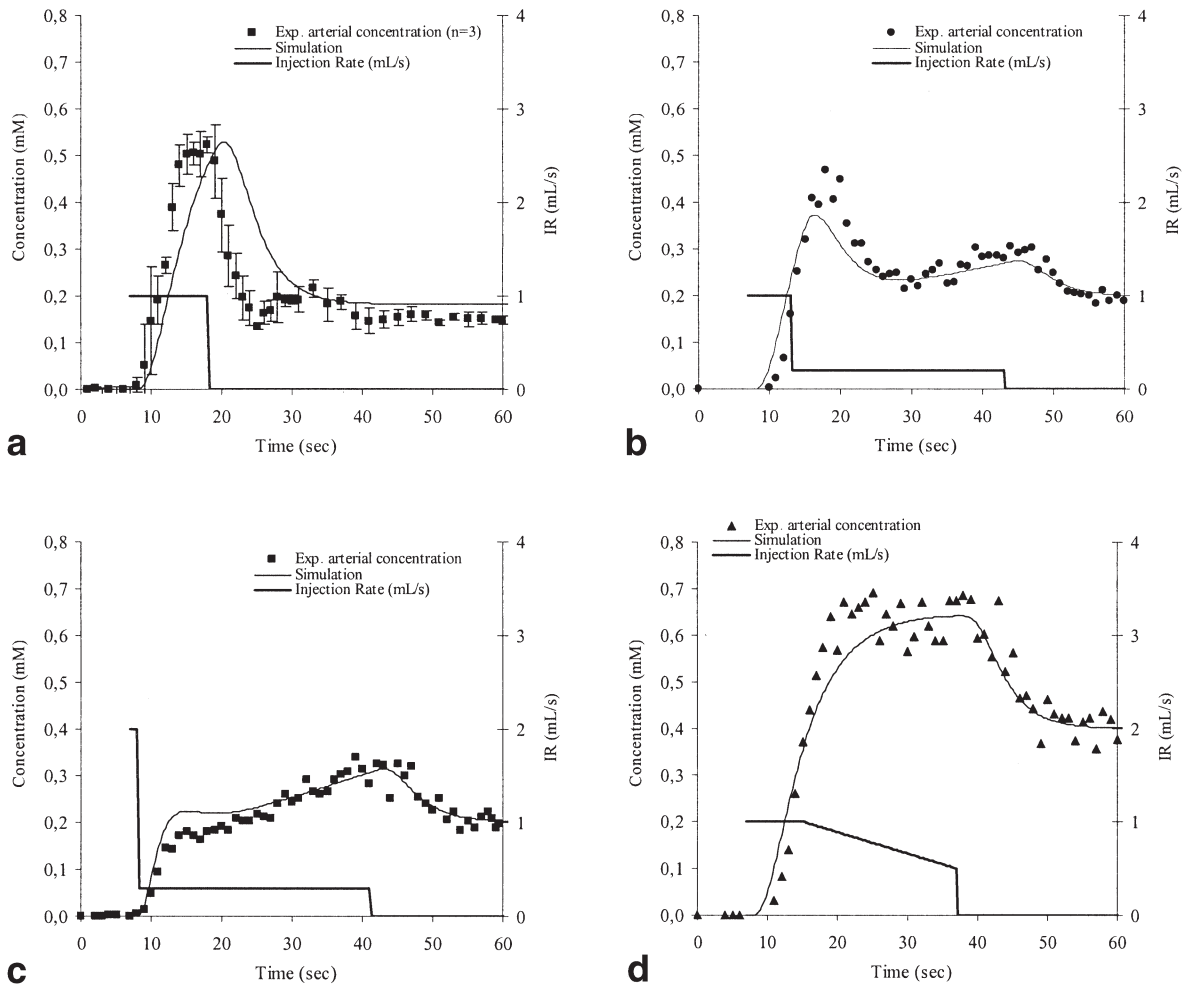


**Figure 5.** First-pass concentration profile as a function of time in pigs after injection of P792 (**a-c**: 13  $\mu\text{mol/kg}$ ; **d**: 26  $\mu\text{mol/kg}$ ). Fitted input data: pig CO = 64.8 mL/second,  $V_s = 63 \text{ mL/kg}^{27}$ ,  $Q_v = 4.2 \text{ mL/second}$ ,  $C_s = 35 \text{ mM}$ ,  $V_v/V_d/V_p/V_g = 14.4/60.4/145/60.4 \text{ mL}$ . An added delay of 7 seconds for the simulated protocol was necessary to fit the curve in the time axis. **a:** Bolus injection of P792: IR = 1 mL/second over 11 seconds. **b:** Biphasic injection protocol of P792: IR = 1 mL/second over 6 seconds, then 0.2 mL/second over 30 seconds. **c:** Biphasic injection protocol of P792: IR = 2 mL/second over 1 seconds, then 0.3 mL/second over 33 seconds. **d:** Ramp injection protocol of P792: IR = 1 mL/second over 8 seconds followed by a ramp of progressive decrease of 1–0.5 mL/second in 22 seconds.

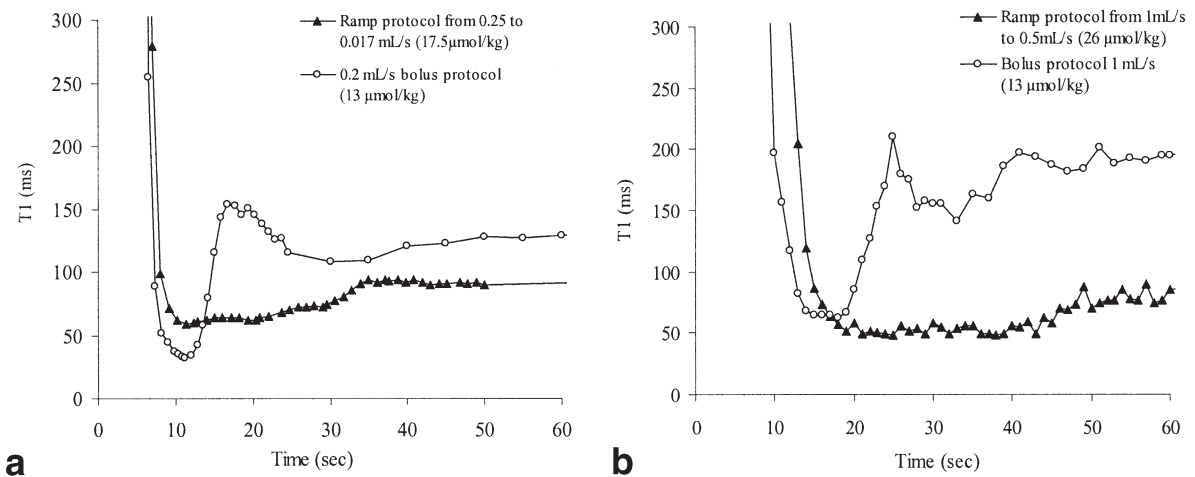


**Figure 6.** Calculated arterial first-pass T1 in **(a)** rabbits and **(b)** pigs for a bolus or a ramp protocol with P792.

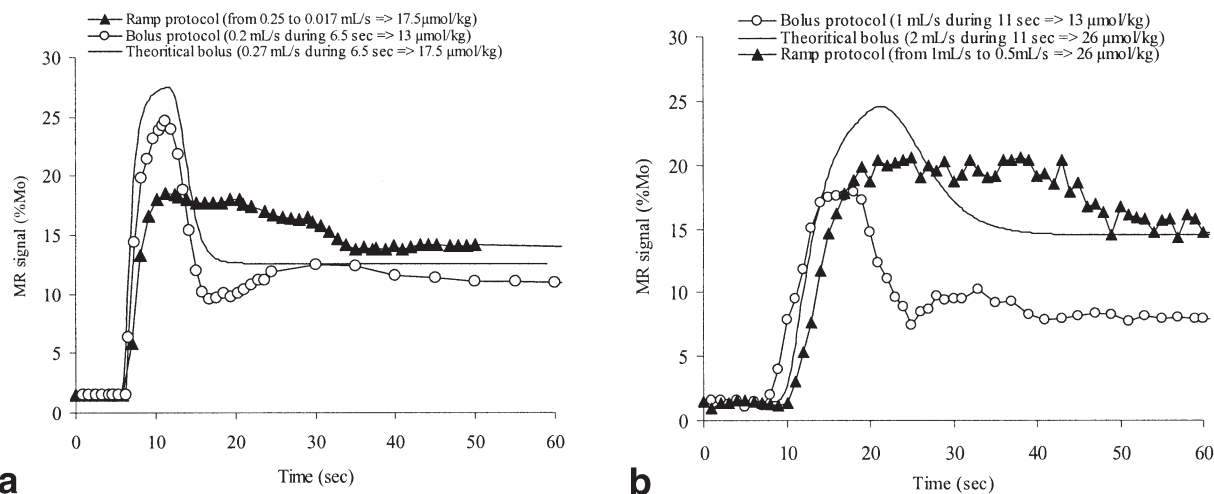


**Figure 7.** Modelized arterial first-pass MR signal in (a) rabbit and (b) pig after i.v. injection of P792. A FLASH T1-weighted sequence was used for signal calculation ( $TR/TE/\alpha = 5.0 \text{ msec}/1.5 \text{ msec}/30^\circ$ ,  $T_{10}/T_{20} = 1.2/0.2 \text{ seconds}$ ,  $r_1/r_2 = 29/65 \text{ mM}^{-1} \cdot \text{s}^{-1}$ ). A simulation of a bolus protocol at the high dosage was added to the graphs to facilitate comparison between the different injection protocols.

concentration. Therefore, it cannot predict the optimum injection rate and duration, which would provide the maximal arterial concentration.

However, in our work we did not evaluate the impact of such an injection protocol on the venous profile. It has been reported that one of the major drawbacks of blood pool agents in MRA is the venous overlay induced by such agents (1). With this ramp protocol, we achieved a constant low T1 for more than 30 seconds. In the arterial curves obtained in pigs, the second pass of the contrast agent is clearly depicted in the arterial system, occurring around 15 seconds after the first pass (Fig. 7b). As a consequence, venous enhancement must occur during the 30-second period of the optimized arterial profile. This could be a limitation for some territories in which arteries and veins are closed (e.g., the peripheral system), but not for coronaries, where venous overlay has not been reported (30).

Previous studies have shown that the contrast-to-noise ratio (CNR) provided by blood pool contrast agents remains high between the vessels and surrounding tissue for several minutes (5). This result suggests that matching the center k-space acquisition with the first pass is not so crucial to achieve a good CNR between the vessel and surrounding tissue. Simultaneously, spatial resolution suffers from a low SNR during the peripheral part of the bolus (31). In this context, high frequencies of the k-space would benefit from being acquired during a high contrast between the vessel and the surrounding tissue. Zheng et al (19) demonstrated that the slow infusion rate of a nonspecific extracellular contrast agent may improve the SNR and the boundary definition of small vessels. Therefore, we suggest that reversed spiral imaging matched with the bolus arrival, as originally developed to optimize T2\* weighting (32,33), may be a way to achieve very high spatial resolution. This hypothesis has been validated in our laboratory by computer simulations (unpublished data).

In conclusion, CE-MRA is currently performed with the use of clinically approved NSAs; however, the dis-

advantage of these small molecules is that they extravasate massively within the surrounding tissues, leading to a decrease in contrast. It has been demonstrated that the use of blood pool contrast agents does not have these limitations. Taking advantage of the blood pool properties of P792 and its high relaxivity is the key to strongly decreasing the blood T1 without increasing the surrounding tissue signal. This prolonged low T1 imaging window could provide high signal intensity ( $T_1 < 80\text{--}100 \text{ msec}$  (2,34)) in the blood for more than 30 seconds. Our results in animals demonstrate that it is possible to optimize the acquisition scheme to obtain a high signal in the blood during a large part of the k-space filling.

This approach makes P792 a promising blood pool contrast agent for CE-MRA and particularly coronary MRI, both of which require high contrast and resolution.

## REFERENCES

1. Prince MR, Grist TM, Debatin J. 2003. Basic concepts. In: Springer, editor. 3D contrast MR angiography. New York: Springer-Verlag. 290 p.
2. Johansson L, Fischer S, Lorenz C. Benefit of T1 reduction for magnetic resonance coronary angiography: a numerical simulation and phantom study. *J Magn Reson Imaging* 1999;9:552-556.
3. Maki J, Prince MR, Londy FJ, Chenevert TL. The effects of time varying intravascular signal intensity and k-space acquisition order on three-dimensional MR angiography image quality. *J Magn Reson Imaging* 1996;6:642-651.
4. Svensson J, Petersson JS, Stahlberg F, Larsson EM, Leander P, Olsson LE. Image artifacts due to a time-varying contrast medium concentration in 3D contrast-enhanced MRA. *J Magn Reson Imaging* 1999;10:919-928.
5. Taupitz M, Schnorr J, Wagner S, et al. Coronary magnetic resonance angiography: experimental evaluation of the new rapid clearance blood pool contrast medium P792. *Magn Reson Med* 2001;46: 932-938.
6. Dirksen MS, Lamb HJ, Kunz P, Robert P, Corot C, De Roos A. Improved MR coronary angiography with use of a new rapid clearance blood pool contrast agent in pigs. *Radiology* 2003;227:802-808.

7. Reiser U. Study of bolus geometry after intravenous contrast medium injection: dynamic and quantitative measurements (chronogram) using an X-ray CT device. *J Comput Assist Tomogr* 1984;8:251-262.
8. Hittmair K, Fleischmann D. Accuracy of predicting and controlling time-dependent aortic enhancement from a test bolus injection. *J Comput Assist Tomogr* 2001;25:287-294.
9. Bae KT, Tran HQ, Heiken JP. Multiphasic injection method for uniform prolonged vascular enhancement at CT angiography: pharmacokinetic analysis and experimental porcine model. *Radiology* 2000;216:872-880.
10. Fleischmann D, Rubin G, Bankier A, Hittmair K. Improved uniformity of aortic enhancement with customized contrast medium injection protocols at CT angiography. *Radiology* 2000;214:363-371.
11. Bae KT, Heiken JP, Brink JA. Aortic and hepatic contrast medium enhancement at CT. Part I. Prediction with a computer model. *Radiology* 1998;207:647-655.
12. Bae KT, Heiken JP, Brink JA. Aortic and hepatic contrast medium enhancement at CT. Part II. Effect of reduced cardiac output in a porcine model. *Radiology* 1998;207:657-662.
13. Fleischmann D, Hittmair K. Mathematical analysis of arterial enhancement and optimization of bolus geometry for CT angiography using the discrete Fourier transform. *J Comput Assist Tomogr* 1999;23:474-484.
14. Corot C, Violas X, Robert P, Port M. Pharmacokinetics of three gadolinium chelates with different molecular sizes shortly after intravenous injection in rabbits: relevance to MR angiography. *Invest Radiol* 2000;35:213-218.
15. Hany T, McKinnon G, Leung D, Pfammatter T, Debatin J. Optimization of contrast timing for breath-hold three-dimensional MR angiography. *J Magn Reson Imaging* 1997;7:551-556.
16. Boos M, Scheffler K, Haselhorst R, Reese E, Frohlich J, Bongartz GM. Arterial first pass gadolinium-CM dynamics as a function of several intravenous NaCl flush and Gd volume. *J Magn Reson Imaging* 2001;13:568-576.
17. Maki J, Prince M, Chenevert T. Optimizing three-dimensional gadolinium-enhanced magnetic resonance angiography. Original investigation. *Invest Radiol* 1998;33:528-537.
18. Schoenberg SO, Lundy FJ, Licato P, Williams DM, Wakefield T, Chenevert TL. Multiphase-multistep gadolinium-enhanced MR angiography of the abdominal aorta and runoff vessels. *Invest Radiol* 2001;36:283-291.
19. Zheng J, Bae KT, Woodard PK, Haacke EM, Li D. Efficacy of slow infusion of gadolinium contrast agent in three-dimensional MR coronary artery imaging. *J Magn Reson Imaging* 1999;10:800-805.
20. Czum JM, Ho VB, Hood MN, Foo TK, Choyke PL. Bolus-chase peripheral 3D MRA using a dual-rate contrast media injection. *J Magn Reson Imaging* 2000;12:769-775.
21. Wendland MF, Saeed M, Yu KK, et al. Inversion recovery EPI of bolus transit in rat myocardium using intravascular and extravascular gadolinium-based MR contrast media: dose effects on peak signal enhancement. *Magn Reson Med* 1994;32:319-329.
22. Port M, Corot C, Raynal I, et al. Physicochemical and biological evaluation of P792, a rapid-clearance blood-pool agent for magnetic resonance imaging. *Invest Radiol* 2001;36:445-454.
23. Port M, Corot C, Rousseaux O, et al. P792: a rapid clearance blood pool agent for magnetic resonance imaging: preliminary results. *MAGMA* 2001;12:121-127.
24. Bourasset F, Dencausse A, Bourrinet P, Ducret M, Corot C. Comparison of plasma and peritoneal concentrations of various categories of MRI blood pool agents in a murine experimental pharmacokinetic model. *MAGMA* 2001;12:82-87.
25. Gross DR. Normal cardiovascular parameters from intact, awake animals. *Animal models in cardiovascular research*. Dordrecht, The Netherlands: Kluwer Academic Publishers; 1994. p 343.
26. Lentner C, editor. Geigy scientific tables: heart and circulation. Vol. V. Basel, Switzerland: CIBA-GEIGY Corporation; 1990.
27. Wolfensohn S, Loeyd M. 1994. *Handbook of laboratory animal management and welfare*. London: Oxford University Press. 400 p.
28. Ruehm SG, Christina H, Violas X, Corot C, Debatin JF. MR angiography with a new rapid-clearance blood pool agent: initial experience in rabbits. *Magn Reson Med* 2002;48:844-851.
29. Bae KT. Peak contrast enhancement in CT and MR angiography: when does it occur and why? Pharmacokinetic study in a porcine model. *Radiology* 2003;227:809-816.
30. Flamm SD, Muthupillai R. Coronary artery magnetic resonance angiography. *J Magn Reson Imaging* 2004;19:686-709.
31. Fain SB, Riederer SJ, Bernstein MA, Huston 3rd J. Theoretical limits of spatial resolution in elliptical-centric contrast-enhanced 3D-MRA. *Magn Reson Med* 1999;42:1106-1116.
32. Börnert P, Aldefeld B, Eggers H. Reversed spiral MR imaging. *Magn Reson Med* 2000;44:479-484.
33. Börnert P, Aldefeld B, Nehrke K, Eggers H. Reversed spiral imaging for coronary MR angiography. In: *Proceedings of the 11th Annual Meeting of ISMRM, Toronto, Canada, 2003*.
34. Zheng J, Li D, Cavagna FM, et al. Contrast-enhanced coronary MR angiography: relationship between coronary artery delineation and blood T1. *J Magn Reson Imaging* 2001;14:348-354.